

Dynamic Analysis of Encastre Beams by Modification of the System's Stiffness Distribution

V. O. Okonkwo, C. H. Aginam, and C. M. O. Nwaiwu

Abstract — Numerical and energy methods are used to dynamically analyze beams and complex structures. Hamilton's principle gives exact results but cannot be easily applied in frames and complex structures. Lagrange's equations can easily be applied in complex structures by lumping the continuous masses at selected nodes. However, this would alter the mass distribution of the system, thus introducing errors in the results of the dynamic analysis. This error can be corrected by making a corresponding modification in the systems' stiffness matrix. This was achieved by simulating a beam with uniformly distributed mass with the force equilibrium equations. The lumped mass structures were simulated with the equations of motion. The continuous systems were analyzed using the Hamilton's principle and the vector of nodal forces $\{P\}$ causing vibration obtained. The nodal forces and displacements were then substituted into the equations of motion to obtain the modified stiffness values as functions of a set of stiffness modification factors. When the stiffness distribution of the system was modified by means of these stiffness modification factors, it was possible to predict accurately the natural fundamental frequencies of the lumped mass encastre beam irrespective of the position or number of lumped masses.

Index Terms— Lagrange's equations; mass lumping; encastre beam; natural frequency; stiffness matrix, finite element analysis.

I. INTRODUCTION

Most real loads on structures are dynamic in nature [1], [2]. To make the analysis simpler the static equivalent of the dynamic load is used [3]-[5]. Dynamic loads cause structures that have mass and elasticity to vibrate [6]. When the exciting force is not continuous, the structure vibrates at one or more of its natural frequencies. The natural frequencies of a structure are peculiar to it. They are dependent on the mass distribution and the stiffness matrix of the structure [7].

The number of independent motions a structure can make is known as its degrees of freedom. Real structures have infinite degrees of freedom. It is however possible to analyse a structure with respect to only few degrees of freedom. This makes the analysis easier. A reduction in the structure's degrees of freedom can be achieved in a number of ways. One such way is by mass lumping. A more popular way of doing this is by breaking the structure into discrete elements and then using the finite element method. The

finite element method has been largely used in structural analysis because of its ability to model complex structures. Its results are not however accurate as errors often arise from poorly known boundary conditions and oversimplification of very complex structural systems [8], [9]. While mass lumping and the finite element method both simplify the structure's mass distribution, mass lumping does so by ignoring the rotational inertia of the masses and treats them as point masses. The finite element method uses a consistency matrix to approximate the mass distribution. The consistency matrix is generated using a chosen shape function. The accuracy of the finite element method is improved upon by dividing the structure into smaller elements or by carefully selecting better shape functions [10], [11]. Another method that makes use of shape functions is the Rayleigh-ritz method. While the Rayleigh-ritz method predicts more accurately the lower natural frequency of vibration, the finite element method gets a better prediction for higher frequencies of vibration [12]. The partial differential equations for the vibration of structures can be obtained using an energy method known as the Hamilton's principle. This is an extension of the principle of least work to accommodate dynamics. Its major drawback is that with the exception of very simple structures formulation of such equations often leads to very complicated mathematics. If, however the continuous mass of the system can be grouped as lumped/point masses, it is easy to analyze the structure using an energy method known as the Lagrange's equations. These equations enable the analysis of structures consisting of lumped masses connected by mass-less elements [13]. With a proper selection of representative masses, the results can be very close to the exact response. When the discretization of the continuous mass is increased by the use of a higher number of lumped masses, the accuracy of the dynamic response improves. Literature is replete with representations of continuous systems with lumped masses connected by mass-less elements [14]. Lin and Tsai [15] modeled a free vibration analysis of a uniform multi-span beam carrying multiple spring mass systems. A numerical model that simulates the vertical dynamic interaction between a lumped massed vehicle and a rail track has also been developed [16]. Its usefulness at offering a simplified solution was exemplified in the works of Katherine Reichi and Daniel Inman when they modeled a meta-structure as a one-dimensional lumped mass [17]. The results from such analysis are usually approximate [18]. In the lumping of masses effort is made to preserve the total mass of the structure even though this alone cannot ensure the quality of the solution [19]. The use of lumped masses (diagonal inertia matrices) simplifies the program coding and results in significant reduction in computer memory and computational effort [20]. Mass lumping of finite elements

Published on November 14, 2020.

V. O. Okonkwo, Nnamdi Azikiwe University, Nigeria.

(e-mail: vo.okonkwo@unizik.edu.ng)

C. H. Aginam, Nnamdi Azikiwe University, Nigeria.

(e-mail: ch.aginam@unizik.edu.ng)

C. M. O. Nwaiwu, Nnamdi Azikiwe University, Nigeria.

(e-mail: cmo.nwaiwu@unizik.edu.ng).

has been applied in acoustics through the use of spectral elements [21]. It has been extended to the dynamic finite element analysis of plates and shells [22]. It is however a general belief that consistent matrix lead to a more accurate solution [23]. The diagonal mass matrix is still employed because of its lesser computational effort. The processes of mathematical modeling and numerical solutions have been transformed by the availability of modeling software [24].

Efforts have also been made at developing simplified models for predicting the natural frequencies of lumped mass structures. The concept of using shear wave in a solid prismatic bar was used by Sule [25] in studying and obtaining approximate natural frequency of vibration of beams under lateral vibration. Osadebe [26] also proposed a model for calculating the natural frequencies of some lumped mass beams after an attempt on finding effective masses for the system. The use of experimental methods through measured data to adjust the analytical mass and synthesize the mass matrix has also been explored [27], [28]. We observe that the approximate methods such as Lagrange's equations (by mass lumping), Rayleigh-ritz and the finite element methods all modify the mass distribution of the structure. While in the use of the Lagrange's equations on lumped masses, a simple redistribution on the basis of the centre of gravity can be done. The Rayleigh-ritz and finite element methods carry out a more complex mass formulation resulting in the consistency matrix. The effort of these methods is to obtain a mass distribution (inertia matrix) representative of the real structure and so produce exact results. In the use of the Lagrange's equations the masses are lumped. Efforts have been made at finding better patterns of lumping that will minimize errors due to the lumping of a continuous mass. Using evenly spaced lumps and increasing the number of lumps is some of the results of such studies. We can see that all the approximate methods hover around the distribution of the mass of the structure; we therefore need to explore the possibility of modification in the structure's stiffness distribution.

A. Mathematical theory

The Lagrange's equations provide a way of analyzing multi-degree of freedom system, a similar approach for continuous structures is the Hamilton's principle.

From this principle the partial differential equation governing the free lateral vibration of a beam can be obtained as[29]:

$$EIu^{IV} + \mu\ddot{u} = 0 \quad (1)$$

where EI is the flexural rigidity of the beam and μ is its mass per unit length. \ddot{u} is the second time derivative of the lateral displacement u . u^{IV} is the fourth derivative of the lateral displacement u with respect to x (an axis parallel to the longitudinal axis of the beam).

By assuming a harmonic vibration and applying the boundary conditions of an encastre beam we obtain the equation of the mode shapes as:

$$\phi_j(x) = \cosh \beta_j x + a_{2j} \sinh \beta_j x - \cos \beta_j x + a_{4j} \sin \beta_j x \quad (2)$$

where

$$a_{2j} = \frac{\cos \beta_j L - \cosh \beta_j L}{\sinh \beta_j L - \sin \beta_j L} \quad (3)$$

$$a_{4j} = \frac{\cosh \beta_j L - \cos \beta_j L}{\sinh \beta_j L - \sin \beta_j L} \quad (4)$$

The values of $\beta_j L$ for the first seven modes of vibration are as presented in Table 1.

TABLE 1: THE FIRST SEVEN NATURAL FREQUENCIES OF AN ENCASTRE BEAM

Mode (j)	$\beta_j L$	$\omega \left(\sqrt{\frac{EI}{\mu L^4}} \right)$
1	4.7300408	22.373286
2	7.8532047	61.672824
3	10.9956078	120.90339
4	14.1371655	199.859448
5	17.2787597	298.55535
6	20.4203522	416.990786
7	23.5619449	555.165247

By taking care of the initial conditions the general solution by mode superposition is therefore [30]:

$$u(x, t) = \sum_{j=1}^{\infty} \phi_j(x) (A_j \cos \omega_j t + B_j \sin \omega_j t) \quad (5)$$

where the constants A_j and B_j can be determined from the initial conditions using the expressions:

$$A_j = \frac{\mu}{M_j} \int_0^l u(x, 0) \phi_j dx \quad (6)$$

$$B_j = \frac{\mu}{M_j \omega_j} \int_0^l \dot{u}(x, 0) \phi_j dx \quad (7)$$

$$M_j = \mu \int_0^l \phi_j^2 dx \quad (8)$$

The eigenfunctions ϕ_j also satisfy certain orthogonality relationships. M_j is the generalized mass for the j^{th} mode of vibration [12].

II. METHODOLOGY

The parameters that determine the vibration of structural systems are the structure's mass distribution and the structure's stiffness [31], [32]. They can be seen in the structure's inertia matrix and stiffness matrix respectively. The roles they play can be seen in the equations of motion of a vibrating system or the structural dynamics' eigenvalue problem. If the j^{th} mode shape ϕ_j and the j^{th} circular frequency ω_j are kept constant, then any variation in mass distribution μ will have a corresponding change in the element flexural rigidity EI .

Two equations were compared. One is the force equilibrium equation written as:

$$\{F\} + [k]\{D\} = \{P\} \quad (9)$$

(where the force vector $\{P\}$ acts at the element's nodes), $\{F\}$ is the vector of fixed end forces generated when nodal displacements are restrained. $[k]$ is the element stiffness matrix and $\{D\}$ a vector of nodal displacements [33].

The second is the equation of motion of a vibrating system written simply as:

$$[m]\{\ddot{u}\} + [k_d]\{u\} = \{P\} \quad (10)$$

where the external force vector $\{P\}$ acts at the element's nodes, $[m]$ is the inertia matrix, $[k_d]$ is the element stiffness matrix and $\{u\}$ a vector of nodal displacements u_1 to u_4 .

Equations (9) can be applied in structural dynamics if the equations for the vector of fixed end moments/forces $\{F\}$ can be formulated. The continuous system was analyzed using the Hamilton's principle and the equations for the fixed end forces $\{F\}$ and nodal displacements $\{D\}$ formulated for any arbitrary segment of a vibrating beam at time $t = 0$. This was then substituted into equation (9) to get the vector of nodal force $\{P\}$ that is causing the vibration.

The stiffness matrix $[K_d]$ in equations (10) was taken as the stiffness matrix of the lumped-mass system. If a vibrating element of the continuous system (beam with continuous mass) and that of a corresponding element of a lumped-mass system (beam with lumped masses) are to be equivalent then their deformation must be equal and the force acting on their nodes $\{P\}$ will also be equal. Therefore:

$$\{D\} = \{u\} \quad (11)$$

A segment of the encastre beam shown in Fig. 1 is being restrained by the fixed end forces F_1 to F_4 . The reduced structure or basic system of the segment is shown in Figure 1b.

From equation (5) the acceleration at any point in the vibrating beam is given by mode superposition as:

$$\ddot{u} = \sum_{j=1}^{\infty} -\omega_j^2 \phi_j(x) (A_j \cos \omega_j t + B_j \sin \omega_j t) \quad (12)$$

From the D'Alembert principle the force on the vibrating beam can be calculated from its inertia force. For an elementary part of the beam at a distance z from the origin this force is $m\ddot{u}dz$.

Using the principle of virtual work and the flexibility method we determine the fixed end forces F_1 to F_4 of the isolated element of the excited beam to be:

$$F_1 = -6 \sum_{j=1}^{\infty} \frac{EIA_j}{L^3(\xi_2 - \xi_1)^3} W_1 \quad (13)$$

$$F_2 = -2 \sum_{j=1}^{\infty} \frac{EIA_j}{L^2(\xi_2 - \xi_1)^2} W_2 \quad (14)$$

$$F_3 = \sum_{j=1}^{\infty} \frac{EIA_j}{L^3(\xi_2 - \xi_1)^3} (6W_1 + \beta_j^3 L^3 (\xi_2 - \xi_1)^3 W_3) \quad (15)$$

$$F_4 = \sum_{j=1}^{\infty} \frac{EIA_j}{L^2(\xi_2 - \xi_1)^2} W_4 \quad (16)$$

where

$$W_1 = \beta_j^3 L^3 \left(\frac{(\xi_2 + \xi_1)(\xi_2^2 - \xi_1^2)}{2} - \frac{2(\xi_2^3 - \xi_1^3)}{3} \right) (-\sinh \beta_j L \xi_1 - a_{2j} \cosh \beta_j L \xi_1 + \sin \beta_j L \xi_1 + a_{4j} \cos \beta_j L \xi_1 + a_{2j} (\beta L (\xi_1 - \xi_2) \cosh \beta_j L \xi_2 + 2 \sinh \beta_j L \xi_2 - \beta_j L (\xi_2 - \xi_1) \cosh \beta_j L \xi_1 - 2 \sinh \beta_j L \xi_1) - a_{4j} (-\beta_j L (\xi_1 - \xi_2) \cos \beta_j L \xi_2 - 2 \sin \beta_j L \xi_2 + \beta_j L (\xi_2 - \xi_1) \cos \beta_j L \xi_1 + 2 \sin \beta_j L \xi_1) + \beta_j L (\xi_1 - \xi_2) \sinh \beta_j L \xi_2 - \beta_j L (\xi_2 - \xi_1) \sinh \beta_j L \xi_1 + \beta_j L (\xi_1 - \xi_2) \sin \beta_j L \xi_2 - \beta_j L (\xi_2 - \xi_1) \sin \beta_j L \xi_1 + 2 \cosh \beta_j L \xi_2 - 2 \cosh \beta_j L \xi_1 - 2 \cos \beta_j L \xi_2 + 2 \cos \beta_j L \xi_1) \quad (17)$$

$$W_2 = \beta_j^3 L^3 \left(\frac{(2\xi_2 + \xi_1)(\xi_2^2 - \xi_1^2)}{2} - \frac{\xi_1(\xi_2 - \xi_1)^2}{2} - (\xi_2^3 - \xi_1^3) \right) (-\sinh \beta_j L \xi_1 - a_{2j} \cosh \beta_j L \xi_1 + \sin \beta_j L \xi_1 + a_{4j} \cos \beta_j L \xi_1) - \left(\frac{\beta_j^2 L^2 (\xi_2 - \xi_1)^2}{2} \right) (\cosh \beta_j L \xi_1 + a_{2j} \sinh \beta_j L \xi_1 + \cos \beta_j L \xi_1 - a_{4j} \sin \beta_j L \xi_1) + \beta_j L (\xi_1 - \xi_2) \sinh \beta_j L \xi_2 - 2\beta_j L (\xi_2 - \xi_1) \sinh \beta_j L \xi_1 + \beta_j L (\xi_1 - \xi_2) \sin \beta_j L \xi_2 - 2\beta_j L (\xi_2 - \xi_1) \sin \beta_j L \xi_1 - 3 \cos \beta_j L \xi_2 + 3 \cos \beta_j L \xi_1 + 3 \cosh \beta_j L \xi_2 - 3 \cosh \beta_j L \xi_1 + a_{2j} (\beta_j L (\xi_1 - \xi_2) \cosh \beta_j L \xi_2 - 2\beta_j L (\xi_2 - \xi_1) \cosh \beta_j L \xi_1 + 3 \sinh \beta_j L \xi_2 - 3 \sinh \beta_j L \xi_1) - a_{4j} (-\beta_j L (\xi_1 - \xi_2) \cos \beta_j L \xi_2 + 2\beta_j L (\xi_2 - \xi_1) \cos \beta_j L \xi_1 - 3 \sin \beta_j L \xi_2 + 3 \sin \beta_j L \xi_1) \quad (18)$$

$$W_3 = \sinh \beta_j L \xi_2 - \sinh \beta_j L \xi_1 - \sin \beta_j L \xi_2 + \sin \beta_j L \xi_1 + a_{2j} (\cosh \beta_j L \xi_2 - \cosh \beta_j L \xi_1) - a_{4j} (\cos \beta_j L \xi_2 - \cos \beta_j L \xi_1) \quad (19)$$

$$W_4 = -6W_1 + 2W_2 - \beta_j^3 L^3 (\xi_2 - \xi_1)^3 (-\sinh \beta_j L \xi_1 - a_{2j} \cosh \beta_j L \xi_1 + \sin \beta_j L \xi_1 + a_{4j} \cos \beta_j L \xi_1) + (\cosh \beta_j L \xi_2 + a_{2j} \sinh \beta_j L \xi_2 + \cos \beta_j L \xi_2 - a_{4j} \sin \beta_j L \xi_2) - (\cosh \beta_j L \xi_1 + a_{2j} \sinh \beta_j L \xi_1 + \cos \beta_j L \xi_1 - a_{4j} \sin \beta_j L \xi_1) \quad (20)$$

$$\xi_1 = x_1/L, \xi_2 = x_2/L \quad (21)$$

To be able to evaluate these equations, there is need to derive an expression for A_j and M_j .

A. Derivation of the expression for A_j for an encastre beam

Consider a uniform encastre beam under the action of its self weight.

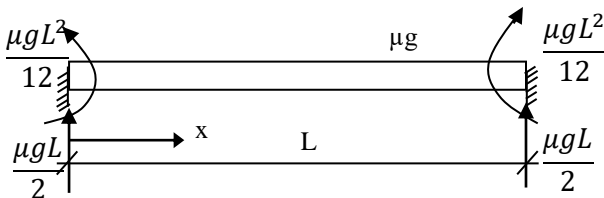


Fig.1. A Uniform fixed-fixed beam under the action of its self weight.

The equation of the bending moment at any distance x from the left support is:

$$M_x = \mu g \left(\frac{Lx}{2} - \frac{x^2}{2} - \frac{L^2}{12} \right) \quad (22)$$

where μ is the mass per unit length of the beam and g is the acceleration due to gravity.

From the equation of elastic curve (beam flexure equation):

$$\frac{M_x}{EI} = \frac{d^2u}{dx^2} \quad (23)$$

By substituting equation (22) into (23) and considering the boundary conditions we obtain the initial deflection of the beam under its self weight as:

$$u(x, 0) = aL \left(\frac{2x^3}{L^3} - \frac{x^4}{L^4} - \frac{x^2}{L^2} \right) \quad (24)$$

where a is dimensionless constant equal to $\mu g L^3 / 24EI$.

Equation (24) is substituted into Equation (6) and (8) to obtain an expression for A_j and M_j .

$$A_j = \frac{a\mu L^2}{M_j} (C_j + a_{2j} D_j) \quad (25)$$

$$M_j = \frac{\mu L}{2} m_j \quad (26)$$

where

$$C_j = \frac{-2(\sinh \beta_j L - \sin \beta_j L)}{\beta_j^3 L^3} + \frac{12(\cosh \beta_j L - \cos \beta_j L)}{\beta_j^4 L^4} - \frac{24(\sinh \beta_j L - \sin \beta_j L)}{\beta_j^5 L^5} \quad (27)$$

$$D_j = \frac{-2(\cosh \beta_j L - \cos \beta_j L)}{\beta_j^3 L^3} + \frac{12(\sinh \beta_j L - \sin \beta_j L)}{\beta_j^4 L^4} - \frac{24(\cosh \beta_j L + \cos \beta_j L - 2)}{\beta_j^5 L^5} \quad (28)$$

$$m_j = 2 + \frac{\sinh \beta L + \sin \beta L}{2\beta L} + a_{2j} \left(\frac{\sinh \beta L}{2\beta L} - 1 \right) + a_{4j}^2 \left(1 - \frac{\sin \beta L}{2\beta L} \right) - 2 \left(\frac{\cosh \beta L \sin \beta L + \sinh \beta L \cos \beta L}{\beta L} \right) + 2a_{4j} \left(\frac{1 - \cos \beta L \cosh \beta L + \sin \beta L \sinh \beta L - \sin^2 \beta L}{\beta L} \right) - 2a_{2j} \left(\frac{\sinh \beta L \sin \beta L + \cosh \beta L \cos \beta L - \sinh^2 \beta L - 1}{\beta L} \right) + 2a_{2j} a_{4j} \left(\frac{\cosh \beta L \sin \beta L - \sinh \beta L \cos \beta L}{\beta L} \right) \quad (29)$$

These equations enable us to calculate the fixed end forces F_1 to F_4 on a segment of a vibrating beam and consequently obtain the nodal forces $\{P\}$. An arbitrary segment of a vibrating element is identified by means of the normalized distances ξ_1 and ξ_2 of its nodes from an origin. ξ_1 and ξ_2 are numbers between 0 and 1.

From equation (9) the vector of nodal forces $\{P\}$ can be obtained from the fixed end forces and nodal displacements as:

$$P_1 = F_1 + \frac{12EI}{l^3} u_1 + \frac{6EI}{l^2} u_2 - \frac{12EI}{l^3} u_3 + \frac{6EI}{l^2} u_4 \quad (30)$$

$$P_2 = F_1 + \frac{6EI}{l^2} u_1 + \frac{4EI}{l} u_2 - \frac{6EI}{l^2} u_3 + \frac{2EI}{l} u_4 \quad (31)$$

$$P_3 = F_3 - \frac{12EI}{l^3} u_1 - \frac{6EI}{l^2} u_2 + \frac{12EI}{l^3} u_3 - \frac{6EI}{l^2} u_4 \quad (32)$$

$$P_4 = F_4 + \frac{6EI}{l^2} u_1 + \frac{2EI}{l} u_2 - \frac{6EI}{l^2} u_3 + \frac{4EI}{l} u_4 \quad (33)$$

EI is the flexural rigidity of the beam. l is the length of the segment and is equal to $x_2 - x_1$ but since the length of the beam l has been normalized and is now equal to unity.

$$l = \xi_2 - \xi_1 \quad (34)$$

u_1, u_2, u_3 and u_4 are the total nodal displacements at the coordinates of the forces F_1, F_2, F_3 and F_4 respectively (see Fig. 1). The total displacement is obtained by totaling the displacements due to all the modes of vibration.

If a segment of a vibrating beam is isolated, it will be in equilibrium with the application of the force vector $\{P\}$. The force vector $\{P\}$ represents the effect of the removed adjoining elements on the isolated segment.

Figure 2a shows a segment of the vibrating continuous beam. The nodal forces on the beam P_1, P_2, P_3 and P_4 are calculated from the equilibrium equations (30 – 33). When the continuous beam is represented by a lumped mass beam (a beam that has its distributed masses lumped at selected nodes), the equivalent segment of the beam is shown in Figure 2b. Just like the real segment the equivalent segment is supported by the same nodal forces P_1, P_2, P_3 and P_4 and has the same nodal displacements as the continuous/real beam. This implies that for the lumped mass beam to be equivalent to the real or continuous beam they must have the same forces and displacements at the nodes.

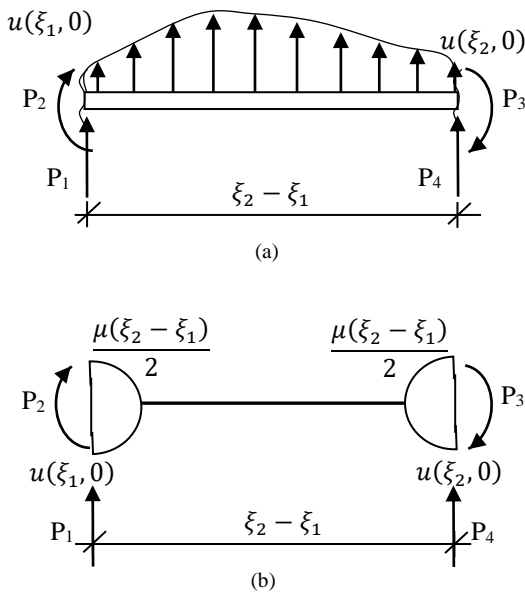


Fig. 2. a) An isolated segment of the laterally vibrating continuous beam showing the nodal forces P_1, P_2, P_3 and P_4 .
b) An equivalent lumped mass segment showing the nodal forces.

Equation (10) is the equation of motion for the lumped mass vibrating beam and the proposed stiffness matrix for the lumped mass segment k_d is:

$$[k_d] = \begin{bmatrix} \frac{12EI}{l^3} \phi_1 & \frac{6EI}{l^2} \phi_2 & -\frac{12EI}{l^3} \phi_3 & \frac{6EI}{l^2} \phi_4 \\ \frac{6EI}{l^2} \phi_2 & \frac{4EI}{l} \phi_1 & -\frac{6EI}{l^2} \phi_4 & \frac{2EI}{l} \phi_3 \\ -\frac{12EI}{l^3} \phi_3 & -\frac{6EI}{l^2} \phi_4 & \frac{12EI}{l^3} \phi_1 & -\frac{6EI}{l^2} \phi_2 \\ \frac{6EI}{l^2} \phi_4 & \frac{2EI}{l} \phi_3 & -\frac{6EI}{l^2} \phi_2 & \frac{4EI}{l} \phi_1 \end{bmatrix} \quad (35)$$

where ϕ_1, ϕ_2, ϕ_3 and ϕ_4 are the stiffness modification factors for lateral vibration. They help redistribute the

stiffness of the lumped mass segment in such a way as to annul the effect of the discretization of the beam due to the lumping of its distributed mass on selected nodes. The inertia matrix of a lumped mass segment is expressed as:

$$[m] = \begin{bmatrix} \frac{\mu(\xi_2 - \xi_1)}{2} & 0 & 0 & 0 \\ 0 & 1 & 0 & 0 \\ 0 & 0 & \frac{\mu(\xi_2 - \xi_1)}{2} & 0 \\ 0 & 0 & 0 & 1 \end{bmatrix} \quad (36)$$

μ is the mass per unit length of the beam.

The vector of nodal acceleration is written as:

$$\{\ddot{u}\} = \begin{Bmatrix} \ddot{u}(\xi_1, 0) \\ \ddot{u}'(\xi_1, 0) \\ \ddot{u}(\xi_2, 0) \\ \ddot{u}'(\xi_2, 0) \end{Bmatrix} = \begin{Bmatrix} -\omega^2 u_{11} \\ -\omega^2 u_{21} \\ -\omega^2 u_{31} \\ -\omega^2 u_{41} \end{Bmatrix} \quad (37)$$

where ω is the fundamental frequency of the vibrating mass, $u_{11}, u_{21}, u_{31}, u_{41}$ are the values of nodal displacements u_1, u_2, u_3 and u_4 when evaluated for the first mode of vibration only.

By substituting equations (35) to (37) into equation (10) and rearranging we obtain:

$$\begin{Bmatrix} \phi_1 \\ \phi_2 \\ \phi_3 \\ \phi_4 \end{Bmatrix} = G^{-1} \begin{Bmatrix} P_1 + \frac{\mu(\xi_2 - \xi_1)}{2} \omega^2 u_{11} \\ P_2 \\ P_3 + \frac{\mu(\xi_2 - \xi_1)}{2} \omega^2 u_{31} \\ P_4 \end{Bmatrix} \quad (38)$$

where

$$G = \begin{bmatrix} \frac{12EI}{l^3} u_{11} & \frac{6EI}{l^2} u_{21} & -\frac{12EI}{l^3} u_{31} & \frac{6EI}{l^2} u_{41} \\ \frac{4EI}{l} u_{21} & \frac{6EI}{l^2} u_{11} & \frac{2EI}{l} u_{41} & -\frac{6EI}{l^2} u_3 \\ \frac{12EI}{l^3} u_{31} & -\frac{6EI}{l^2} u_{41} & -\frac{12EI}{l^3} u_{11} & -\frac{6EI}{l^2} u_{21} \\ \frac{4EI}{l} u_{41} & -\frac{6EI}{l^2} u_{31} & \frac{2EI}{l} u_{21} & \frac{6EI}{l^2} u_{11} \end{bmatrix} \quad (39)$$

Equation (38) is a mathematical expression for calculating the four stiffness modification factors for a segment of fixed-fixed beam under lateral vibration.

Equation (5) was used to evaluate the total displacements u_1 to u_4 at the nodal points of a segment of the vibrating encastre beam. Though the equations represent the summation of an infinite series, an evaluation of the first few terms provides values of very good precision.

The values of the fixed end forces F_1, F_2, F_3 and F_4 are evaluated using the equations (13 – 16). By substituting the calculated fixed end forces into the equations for nodal forces (equations 30 – 33) the nodal forces P_1, P_2, P_3 and P_4 are obtained.

The nodal displacements and the calculated nodal forces P_1 to P_4 are substituted into equation (38) in order to obtain the stiffness modification factors ϕ_1, ϕ_2, ϕ_3 and ϕ_4 . A

numerical demonstration of these steps is presented below (see Table 2). For clarity the calculations will be presented in a tabular form. Using the methods presented in Table 2 the values of stiffness modification factors at different values of ξ_1 and ξ_2 for the lateral vibration of the beam can be obtained.

TABLE 2: CALCULATION OF THE STIFFNESS MODIFICATION FACTOR FOR AN ELEMENT POSITIONED AT $\xi_1 = 0, \xi_2 = 0.5$ ON A ENCASTRE BEAM UNDER LATERAL VIBRATION

$\xi_1 = 0, \xi_2 = 0.5$					
j	A_j	F_{1j}	F_{2j}	F_{3j}	F_{4j}
1	-0.039836	-6.073543	-0.434916	-2.210428	0.264158
2	0	-0.000001	-0	-0	0
3	-0.000597	0.080615	-0.082557	-1.668553	0.164574
4	0	0	0	-0	0
5	-0.000062	-0.008475	0.024225	-0.635416	0.035146
6	0	0	0	0	0
7	-0	0.000004	-0.000019	-0.000679	0.000030
Total	-6.001400	-0.493267	-4.515076	0.463908	

j	A_j	u_{1j}	u_{2j}	u_{3j}	u_{4j}
1	-0.039836	-0.063266	0	0	-0
2	0	0	-0	0	0
3	-0.000597	0.000840	0	0	-0
4	0	0	0	0	0
5	-0.000062	-0.000088	0	0	-0.
6	0	0	0	0	0
7	-0	0	0	0	0
Total	-0.062514	-0	0	0	-0

$u_{11} = -0.06326607054284$ $u_{31} = 0$
 $u_{21} = 0.00000000631491$ $u_{41} = -0.00000002080837$
 From Eqs. (13) to (16)
 $F_1 = 6.00139983367608$ $F_3 = 4.51507647183599$
 $F_2 = 0.49326746228404$ $F_4 = -0.46390779670347$
 From Eqs. (30) – (33)
 $P_1 = 1.838594375614049 \times 10^{-5}$
 $P_3 = 10.51647612165263$
 $P_2 = -1.00708240975866$
 $P_4 = -1.96425774956910$
 From Eq. (37) taking $EI = 1$
 $\phi_1 = 1.303552$ $\phi_3 = 1.731522$
 $\phi_2 = 0.663259$ $\phi_4 = 1.293649$

The values in the tables were written at 7 significant figures except for the summary which are at 14 decimal points to capture the values that are near zero.

Using the methods presented in Table 2 the values of stiffness modification factors at different values of ξ_1 and ξ_2 for the lateral vibration of the beam can be obtained.

III. NUMERICAL APPLICATION AND DISCUSSION OF RESULTS

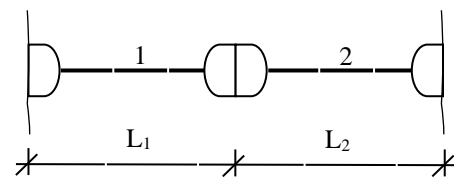
The lumped mass beam of Fig. 3a (if rigidly restrained at both ends) was analyzed at different values of L_1 and L_2 to obtain the values of the fundamental frequency. The analysis was done first with the Lagrange's equations, and then by using the method presented in Table 2, the stiffness factors were obtained and used with the Lagrange's equations to get an improved result. Finally, the beam was analysed using the finite element method. Their results are presented in Table 3.

Table 3 shows that the values of the calculated frequency vary with the relative values of L_1 and L_2 . When Lagrange's equations were used without stiffness modification factors the obtained values differed considerably. The difference between the highest and the lowest values was 48.121. This was obtained when $L_1 = 1/8, 7/8$ and $1/2$. The result from

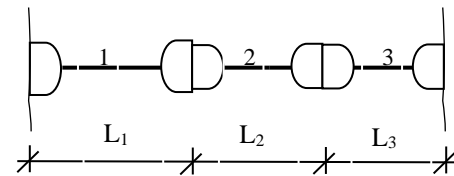
finite element analysis was better even though it exhibited the same trend. The difference between the highest and lowest obtained values was 9.298 and where obtained at same positions as that from the use of the finite element method. The application of stiffness modification factors gave approximately the exact result of 22.373.

TABLE 3: CALCULATED VALUES OF THE FUNDAMENTAL FREQUENCY FOR THE BEAM OF FIGURE 3A

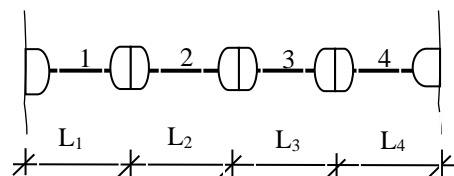
s/n	L_1/L	L_2/L	Fundamental frequency $\omega \left(\sqrt{\frac{EI}{\mu L^4}} \right)$		
			Lagrange's equations without ϕ	Lagrange's equation with ϕ	Finite Element Method (FEM)
1	1/8	7/8	67.717	22.373	32.034
2	2/8	6/8	30.170	22.373	25.307
3	3/8	5/8	21.588	22.373	23.242
4	4/8	4/8	19.596	22.373	22.736
5	5/8	3/8	21.588	22.373	23.242
6	6/8	2/8	30.170	22.373	25.307
7	7/8	1/8	67.717	22.373	32.034



(a)



(b)



(c)

Fig. 3: Some lumped mass encastre beams.

The trend is better appreciated by taking a look at the plot of the fundamental frequency against L_1/L in Fig. 4.

The plots in Fig. 4 are all symmetrical about $L_1/L = 1/2$. This is expected because the lumping of the mass of the beam is symmetrical about the beam centre. The fixed supports are also of equal distance from the beam centre. From the plots of Fig. 4 we observe that it is possible to obtain a good approximate of the exact value of the fundamental frequency by a careful selection of the position of the lumped mass. The calculated values of the fundamental frequency were best near $L_1/L = 3/8$ and $5/8$ for the Lagrange's equations and $L_1/L = 1/2$ for the finite element method.

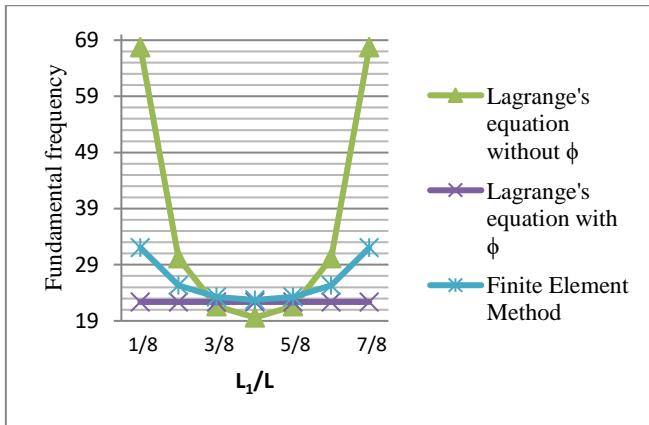


Fig. 4. Plot of fundamental frequency against L_1/L for the beam of Fig. 3a

A single factor analysis of variance was used to compare the values obtained from the use of the Lagrange's equation (with stiffness modifications factors) and that from the finite element method. The results gave $F_{crit} = 4.747$, $F = 6.440$ and $P\text{-value} = 0.026$. Since $F_{crit} < F$ and $P\text{-value} < 0.05$, we accept that there was significant improvement in the results obtained by the application of the modification factors.

By increasing the number of lumps to two as shown in Figure 3b, we now have two independent variables L_1 and L_2 . The value of L_3 can be obtained the moment the values of L_1 and L_2 are specified hence it is not independent. The results of the dynamic analysis of the beam of Fig. 3b is presented in Table 4.

TABLE 4: CALCULATED VALUES OF THE FUNDAMENTAL FREQUENCY FOR THE BEAM OF FIGURE 3B

S/ N	L_1/L	L_2/L	L_3/L	Fundamentalfrequency $\omega(\sqrt{\frac{EI}{\mu L^4}})$		
				Lagrange's equations without ϕ	Lagrange's equation with ϕ	Finite Element Method (FEM)
1	1/9	1/9	7/9	35.558	22.374	26.168
2	1/9	2/9	6/9	24.607	22.373	23.683
3	1/9	3/9	5/9	21.067	22.373	22.781
4	1/9	4/9	4/9	21.084	22.373	22.640
5	1/9	5/9	3/9	24.685	22.373	23.104
6	1/9	6/9	2/9	35.888	22.373	24.469
7	1/9	7/9	1/9	76.843	22.374	27.589
8	2/9	1/9	6/9	24.463	22.373	23.681
9	2/9	2/9	5/9	21.288	22.373	22.753
10	2/9	3/9	4/9	21.366	22.373	22.510
11	2/9	4/9	3/9	24.658	22.373	22.671
12	2/9	5/9	2/9	32.472	22.373	23.271
13	2/9	6/9	1/9	35.888	22.373	24.469
14	3/9	1/9	5/9	20.333	22.373	22.755
15	3/9	2/9	4/9	20.140	22.373	22.465
16	3/9	3/9	3/9	22.045	22.373	22.465
17	3/9	4/9	2/9	24.678	22.373	22.671
18	3/9	5/9	1/9	24.685	22.373	23.104
19	4/9	1/9	4/9	19.211	22.373	22.523
20	4/9	2/9	3/9	20.140	22.373	22.465
21	4/9	3/9	2/9	21.366	22.373	22.510
22	4/9	4/9	1/9	21.084	22.373	22.640
23	5/9	1/9	3/9	20.333	22.373	22.755
24	5/9	2/9	2/9	21.288	22.373	22.753
25	5/9	3/9	1/9	21.067	22.373	22.781
26	6/9	1/9	2/9	24.463	22.373	23.681
27	6/9	2/9	1/9	24.607	22.373	23.683
28	7/9	2/9	1/9	35.558	22.374	26.168

From Table 4 it would be seen that the application of the Lagrange's equations with stiffness modification factors gave the exact value of the fundamental frequency. It is also worthy of note that the value obtained was not dependent on the relative values of L_1 , L_2 and L_3 . The values of the fundamental frequency ω obtained with the deployment of Lagrange's equations without the stiffness modification factors however varied with the relative values of L_1 and L_2 . This same observation was also noticed in the results from a finite element analysis. The effect of the relative variation of L_1 and L_2 on the fundamental frequency was studied by carrying out a two-way analysis of variance ANOVA on the values in table 3 for L_1/L and L_2/L of 1/9 to 4/9. The result was presented in Table 5.

TABLE 5: ANALYSIS OF VARIANCE ANOVA RESULTS FOR THE VALUES FROM THE USE OF LAGRANGE'S EQUATIONS
Anova: Two-Factor Without Replication

SUMMARY	Count	Sum	Average	Variance
Row 1	4	102.316	25.579	47.02946
Row 2	4	91.775	22.94375	3.492526
Row 3	4	91.548	22.887	4.898486
Row 4	4	81.801	20.45025	0.957411
Column 1	4	99.372	24.843	56.26442
Column 2	4	88.08	22.02	3.587806
Column 3	4	88.477	22.11925	2.929734
Column 4	4	91.511	22.87775	4.290174
ANOVA				
Source of Variation	SS	df	MS	F
Rows	52.654	3	17.55133	1.06327
Columns	20.57126	3	6.857086	0.415406
Error	148.5624	9	16.50693	
Total	221.7877	15		

In carrying out the ANOVA the rows represented L_1/L and the columns the different values of L_2/L . From Table 5, it would be seen that neither L_1/L nor L_2/L was found significant. Their p-values were 0.412 and 0.746 respectively and which are more than 0.05. This suggests that an interaction between them may be largely responsible for any observed variation in the values of the fundamental frequencies obtained. The interaction plots for L_1/L and L_2/L (see Fig. 5) however showed consideration interactions. The lines $L_1/L = 1/9, 2/9, 3/9$ and $4/9$ were not parallel and intercepted at some points. The graphs revealed that it is possible to obtain the exact value of the fundamental frequency by a careful selection of the values of L_1 and L_2 . This is evident because the lines for different values of L_1/L all crossed the horizontal line for the frequency of 22.373 at some point. The same is observed for the values obtained from a finite element analysis at different values of L_1/L and L_2/L presented in Fig. 6.

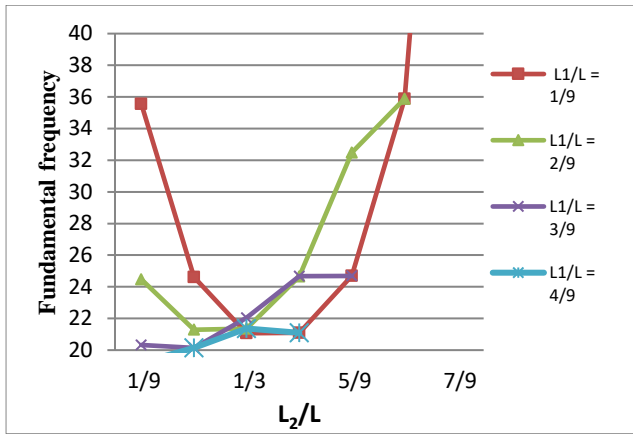


Fig. 5. Plots of fundamental frequency against L_2/L for different values of L_1/L obtained from the lumped mass analysis of the encastre beam of Fig. 3b.

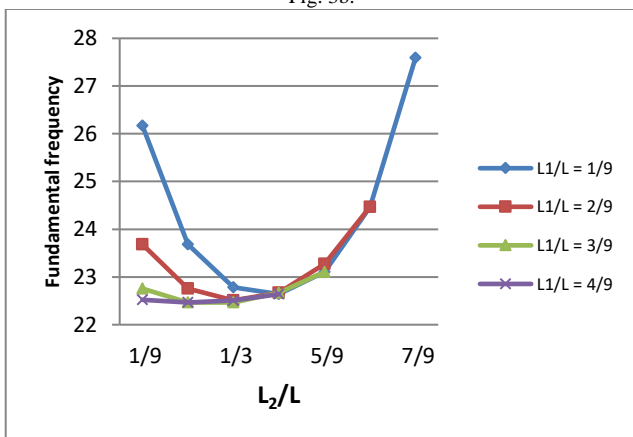


Fig. 6. Plots of fundamental frequency against L_2/L for different values of L_1/L obtained from the finite element analysis of the encastre beam of Fig. 3b.

The lines in Fig. 6 are not parallel and intercept at some points. However the values of L_2/L that gave the best approximation of the fundamental frequency was in the neighbourhood of $2/9$ at $L_1/L = 3/9$ and $4/9$. At higher values of L_2/L the results deviated more from the exact value.

The introduction of more lumps in Fig. 3c led to similar results. But unlike in Fig. 3b, the number of independent variables rose to three. They are L_1/L , L_2/L and L_3/L . The value of L_4/L is defined once the values of the others are known. A similar interaction plot of the type shown in Fig. 5 would result in bogus surface plots. Hence, we decided to compute the average value for fundamental frequency obtained at different values of L_1/L , L_2/L , L_3/L and L_4/L . The plots are presented in Fig. 7.

The graphs for span L_1 and Span L_4 are the same due to symmetry. The same applies to graphs for span L_2 and span L_3 . From the graphs we observe that the results from finite element analysis gave average fundamental frequencies that are close to the exact frequency irrespective of the values of the span lengths. The values of the span L_1 and L_4 for best fit were such that made L_1/L and L_4/L approximately $1/4$. For the application of Lagrange's equations on lumped masses the best fit was obtained when L_1/L and L_4/L are approximately $5/16$. The response varied more and so depends more on the relative values of the spans L_1 , L_2 , L_3 and L_4 .

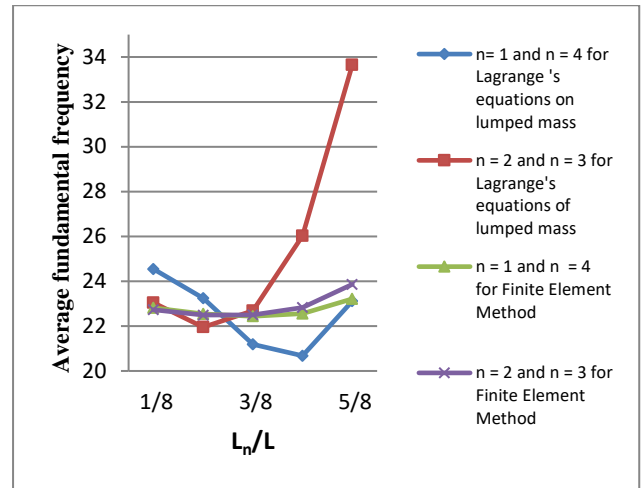


Fig. 7. A graph of average fundamental frequency against the relative span length L_1/L , L_2/L , L_3/L and L_4/L for the beam of Fig. 3c.

IV. CONCLUSION

It would be observed that the natural frequencies obtained from the use of Lagrange's equations on the continuous system that had been represented as lumped masses had some measure of errors as seen from its comparison with the exact results. The error was more when the spacing between the lumped masses was higher and when the number of lumps was less. However, when the stiffness of the system was modified using the stiffness modification factors, the use of Lagrange's equations were able to predict accurately the fundamental frequencies hence their percentage errors were zero. The rigors involved in the manual calculation of the stiffness modification factors can be substantially reduced by writing a simple computer program for its execution.

From this work we can infer that:

- 1) An accurate dynamic response from a lumped mass encastre beam can be obtained by a modification in the stiffness composition of the system.
- 2) The values of the calculated stiffness modification factors obtained for each segment are not equal as shown in Table 1. This implies that no linear modification of the stiffness distribution of lumped mass encastre beams under lateral vibration can cause them to be dynamically equivalent to the continuous beams.
- 3) It is possible to obtain an exact response from the lumped mass beam through a careful selection of the position and spacing between lumps.

The improvement in the accuracy of the estimated fundamental frequencies did not depend on the location of mass lumps or the number of lumped masses. The stiffness modification factors helped to correct the error introduced in the system by mass discretization or lumping.

This is a work on the modification of a structure's stiffness in order to improve the results from a dynamic analysis a continuous beam represented as a lumped mass structure. Encastre beams (fixed at both ends) were used as a first demonstration but it can be easily implemented in beams of other restraints (fixed-pinned, fixed-free etc) and similar equations generated and with corresponding stiffness modification factors. These will reveal the relationship between the modification factors and the end restraints and since the stiffness modification factors are generated with

respect to segments of these beams we will observe that they depend on the restraint provided by adjoining elements and hence on their stiffness. These will lay the foundation for the analysis of frames simply by lumping their continuous masses at their joints and then using modification factors evaluated as a function of the joint rigidities of member elements to carry out dynamic analysis of the frame with no compromise on the accuracy of results obtained.

ACKNOWLEDGMENT

We want to specially thank Late Prof I. O. Onyeyili, the former deputy vice-chancellor of Nnamdi Azikiwe University for his technical support to us in carrying out this research.

REFERENCES

- [1] Choi W. S, Park G. J, "Transformation of dynamic loads into equivalent static loads based on modal analysis", *International Journal for Numerical Methods in Engineering*. Vol 46, Iss. 1, pp 29–43. 1999 [https://doi.org/10.1002/\(SICI\)1097-207\(19990910\)46:1<29::AID-NME661>3.0.CO;2-D](https://doi.org/10.1002/(SICI)1097-207(19990910)46:1<29::AID-NME661>3.0.CO;2-D).
- [2] Choi W. S, Park K. B., Park G. J, "Calculation of Equivalent Static Loads and its Application", *Transactions, SMiRT 16*, Washington DC. 2001. <https://repository.lib.ncsu.edu/bitstream/handle/1840.20/30457/B1111.pdf?sequence=1&isAllowed=y>.
- [3] Kim H., Kim E., Cho M., "Transformation of Dynamic Loads in Equivalent Static Load based on the stress constraint conditions", *Journal of the Computational Structural Engineering*, Vol 26 (2013). DOI:10.7734/COSEIK.2013.26.2.165
- [4] Kim H., Kim E., Cho M., "Study on the Structural Optimization based on Equivalent Static Load under Dynamic Load", *Journal of the Computational Structural Engineering*, Vol 26. (2014) pp 421-427. DOI:10.7734/COSEIK.2014.27.5.421
- [5] Park K. J., Lee J. N., Park G. J., "Structural Shape Optimization using equivalent static loads transformed from dynamic loads", *International Journal of Numerical Methods in Engineering*, Vol. 63, Issue 4 pp 589-602, 2005, DOI:10.1002/nme.1295.
- [6] Rajasekaran, S., *Structural Dynamics of Earthquake Engineering: Theory and Application using Mathematica and Matlab*, Woodhead Publishing Limited Cambridge, 2009.
- [7] Ezeokpube, G. C., "Dynamic Response of Frames with stiffened joints", M.Eng Thesis University of Nigeria Nsukka, 2002.
- [8] De Basabe J. D., Sen M. K., "A comparison of finite difference and spectral-element methods for elastic wave propagation in media with a fluid-solid interface", *Geophysical Journal International*, vol. 200, Issue, 1 pp 278 – 298, 2015. <https://doi.org/10.1093/gji/ggu389>.
- [9] Perumal P., "A review on Polygonal/Polyhedral finite element methods", *Mathematical Problems in Engineering*, vol. 2018, pp 1 – 23, 2018. <https://doi.org/10.1155/2018/5792372>.
- [10] Beaurepaire, P and Schueller, G. L., "Modelling of the Variability of fatigue Crack growth using cohesive zone element", *Engineering Fracture Mechanics* Vol 78 Issue 12 pp 2399-2413, 2011. Elsevier. DOI: 10.1016/j.engfracmech.2011.05.011.
- [11] Tornabene, F., Nicholas, Fanluzzi, Uberlini, F., Erasmo, V., "Strong Formulation Finite Element Method based on Differential Quadrature: A Survey", *Applied Mechanics Review* Vol 67 pp 1-50, 2015, ASME. <https://doi.org/10.1115/1.4028859>.
- [12] Tauchert, T. R., *Energy Principles in Structural Mechanics*, International Student Edition, McGraw-Hill Kogakusha Ltd Tokyo, 1974.
- [13] Ahmad, Z. and Campbell, J., "Development of Two-dimensional Solver Code for Hybrid Model of Energy absorbing system", *International Journal of Physical Sciences*, vol 8 (13), pp 510 – 525, 2013. DOI: 10.5897/IJPS12.584.
- [14] Ashithamol S., Yedu K. M., Nithin W., "Study on mass lumping methods of framed structures", *International Journal of Engineering Research and Technology*, vol. 5, Issue 9, pp 253 – 257, 2016. <http://dx.doi.org/10.17577/IJERTV5IS090271>.
- [15] Lin HY., Tsai YC, "Free Vibration Analysis of uniform multi-span beam carrying multi spring-mass systems", *Journal of Sound and Vibration*, Vol 302, Issue 3, pp 442 – 456, 2007. <https://doi.org/10.1016/j.jsv.2006.06.080>.
- [16] Zhai, W., Cai, Z., "Dynamic Interaction between a lumped mass vehicle and a discretely supported continuous rail track", *Computers and Structures* Vol. 63, Issue 5. pp 987 – 997. [https://doi.org/10.1016/S0045-7949\(96\)00401-4](https://doi.org/10.1016/S0045-7949(96)00401-4).
- [17] Reichi, K. K. and Iman, D. J., "Lumped mass model of a 1-dimensional metastructure for vibration suppression with no additional mass", *Journal of Sound and Vibration*, Vol. 403. pp 75-89. 2017. <https://doi.org/10.1016/j.jsv.2017.05.026>.
- [18] Torkian, B. B., Chandran, P., Ratnagar B. J., Miller R. and Lu S., "Validation of lumped mass stick models for surface founded structures", *Transactions, SMiRT-22*, San Francisco, California, USA. pp 1 – 11. 2013.
- [19] Iyer, R., 1993, Error Estimation and Adaptive Refinements for Finite Element Analysis of Structures, PhD Thesis, Indian Institute of Science, Bangalore.
- [20] Ma L., Liu J., Jia X., Yan Y., "Lumped mass matrix of three-node beam element", *Advanced Materials Research*, vol. 616-618, pp 1969 – 1973. 2012. DOI: 10.4028/www.scientific.net/AMR.616-618.1969.
- [21] Cohen G., Fauqueux S., "Mixed finite elements with mass-lumping for the transient wave equation", *Journal of Computational Acoustics*, vol 8(1), (2000), pp 171-188. DOI: 10.1016/S0218-396X(00)00011-X.
- [22] Iyer R., Pilani, G. S. and Rao, T. V., "Influence of Mass Representation Schemes on Vibration Characteristics of Structures", *Technical Journal: Aerospace Engineering*, The Institute of Engineers Vol 84, pp 19 – 26. 2003.
- [23] Nandi, S.K. and Bosu, S., "Effect of Mass Matrix Formulation Schemes on Dynamics of Structures", *International ANSYS Conference Proceeding*, www.ansys.com, paper 50, 2004.
- [24] Ferro R. M., Ferreira W. G., Calenzani A. F. G., "Dynamic Analysis of support frame structures of rotating machinery", *Global Journal of Research in Engineering*, vol. 14, Issue 5, pp 27-31. 2014 https://globaljournals.org/GJRE_Volume14/4-Dynamic-Analysis-of-Support.pdf.
- [25] Sule, S., "Approximate Method for the determination of natural frequencies of a Multi-degree of freedom beam system", *Nigerian Journal of Technology*, Vol 30, No 2, pp 1 – 6. 2011 <https://www.ajol.info/index.php/njt/article/view/123519>.
- [26] Osadebe, N. N., "An Improved MDOF Model Simulating some Systems with distributed mass", *Journal of University of Science and Technology Kumasi*, Vol. 19, pp. 56-61, 1999.
- [27] Ross R. G., "Synthesis of stiffness and mass matrices from experimental vibration modes", *SAE Transactions*, vol. 80, section 4, (1971) pp 2627 – 2635. <https://doi.org/10.4271/710787>.
- [28] Cha P. D., De Pillis L. G., "Model Updating by adding known masses, International Journal for Numerical Methods in Engineering", vol. 50, pp 2547 – 2571. 2001 <https://doi.org/10.1002/nme.136>.
- [29] Torabi K, Afshari H, Zafari E., "Transverse Vibration of Non-uniform.
- [30] Euler-Bernoulli Beam using Differential Transform Method (DTM)", *Applied Mechanics and Materials*, vols 110 – 116 (2012) pp 2400 – 2405. DOI:10.4028/www.scientific.net/AMM.110-116.2400.
- [31] Thomson, W. T. and Dahleh M. D., *Theory of Vibrations with Applications*, 5th Edition, Prentice Hall New Jersey, 1998.
- [32] Gao, W., "Natural frequency and mode shape analyses of structures with uncertainty", *Mechanical Systems and Signal Processing*, vol. 21, issue 1, pp 24 – 39, 2007, Elsevier. DOI: 10.1016/j.ymsp.2006.05.007.
- [33] Kumar A., Jaiswal H., Jain R., Patil P. P., "Free vibration and material mechanical properties influence based frequency and mode shape analysis of transmission gearbox casing", 12th Global Congress on Manufacturing and Management, *Procedia Engineering* 97, (2014) pp 1097 – 1106. <https://doi.org/10.1016/j.proeng.2014.12.388>.
- [34] Hibbeler R. C., *Structural Analysis*, 8th Edition, Person, 2012.